Original Research

Gradient-Echo Perfusion Imaging of Musculoskeletal Abnormalities with Contrast-Enhanced Two-Dimensional Fat-Saturation FLASH

Orhan Konez, MD • Kostaki G. Bis, MD • Ali Shirkhoda, MD • Anil N. Shetty, PhD
Mehmet Gürgün, MD • Richard Wilcox, MD • Ronald Irwin, MD

The objective of this study was to evaluate the utility of MR perfusion imaging of various musculoskeletal lesions with a contrast-enhanced two-dimensional fat saturation fast low angle shot (FLASH) sequence and to assess the potential of this technique for distinguishing malignant from benign conditions. Thirty-six musculoskeletal lesions were studied at 1.5 T. The signal intensity of the lesions, adjacent artery, muscle, bone marrow, and fat were plotted against time. The time to peak enhancement, time to maximum signal intensity, percent enhancement, rate of peak enhancement, and rate of enhancement parameters were calculated. Because of a significant overlap between malignant and benign conditions, accuracy rates were lower than reported previously. The best parameter based on these values was the rate of peak enhancement (sensitivity, 84.6%; specificity, 65.2–66.6%; positive predictive value, 57.8–68.7%). Fat saturation gradient-echo MR perfusion imaging allows for a rapid assessment of the vascularity of musculoskeletal pathology; however, a significant overlap persists between malignant neoplasms and several benign conditions.

Index terms: Gradient echo • Magnetic resonance • Perfusion • Musculoskeletal

JMRI 1997; 7:895–902

Abbreviations: AVN = avascular necrosis, FA = flip angle, FLASH = fast low angle shot, FOV = field of view, FP = first pass, NPV = negative predictive value, PPV = positive predictive value, ROI = region of interest, SE = spin echo, SI = signal intensity, STIR = short-inversion-time inversion recovery.

From the Departments of Diagnostic Radiology (O.K., K.G.B., A.S., A.N.S., M.G., R.W.) and Orthopedic Surgery (R.I.), William Beaumont Hospital, 3601 West, 13 Mile Road, Royal Oak, MI 48073. Received June 5, 1996; revision received February 7, 1997; second revision requested March 21; second revision received April 16; accepted April 22. Research supported by a Grant RI-93-01 from the William Beaumont Hospital Research Institute. **Address reprint requests to** K.G.B.

PREVIOUS STUDIES have reported that dynamic contrast-enhanced MRI techniques are useful for the differentiation of malignant from benign tumors, differentiation of viable from nonviable (necrotic) portions of neoplasms, prediction of response of musculoskeletal neoplasms to preoperative chemotherapy and monitoring the response to chemotherapy (1–9). Some studies also have shown an application of these techniques to non-neoplastic conditions such as avascular necrosis (AVN) and rheumatoid arthritis (10,11).

The main goal of these techniques is to assess the dynamic enhancement profiles of pathologic musculoskeletal tissues by using relatively fast MRI in an attempt to characterize musculoskeletal lesions. The exact meaning of "dynamic" imaging, however, has varied somewhat. Some investigators have used relatively slower sequences such as conventional spin echo (SE) including, for example, baseline, 1-, 5-, and 10-minute images (4,9,10). Others have used more rapid sequences such as fast low angle shot (FLASH) or turbo FLASH to assess the first pass (FP) enhancement of musculoskeletal lesions (1).

The accuracy for assessing the malignant nature of musculoskeletal neoplasms using slope values has been fairly consistent, ranging from 76% (1) to 79.7% (2). The accuracy for differentiating inflammatory from neoplastic conditions has been reported to be 88% (6).

To our knowledge, dynamic contrast-enhanced MR techniques have not been coupled with fat suppression for the evaluation of musculoskeletal lesions. In this study, our goal was to reassess previous findings in a wide variety of musculoskeletal lesions using a FLASH sequence coupled with fat suppression. This technique might improve the soft tissue contrast resolution and eliminate the need for data subtraction between precontrast and postcontrast dynamic images and associated misregistration artifacts.

• MATERIALS AND METHODS

The research project was approved by the institutional review board of the hospital. Informed consent was obtained from all patients.

Table 1
Benign Tumors (1–6) and Conditions (7–22)

	TP	TM	PE	RPeakE	RE
1. Enchondroma 1	56	119	169.0	52.7	29.6
2. Enchondroma 2	10	30	134.2	226.5	143.8
3. Enchondroma 3	10	91	77.7	99.2	41.6
4. Intraosseous lipoma	7	35	62.3	97.2	89.2
5. Intramuscular lipoma	28	112	71.3	91.8	34
6. Giant cell tumor of tendon sheet	0	0	100.0	142.8	142.8
7. Eosinophilic granuloma	0	56	233.1	471.0	181.8
8. Lymphohistiocytic granulomatous lesion	7	49	166.6	740.1	158.7
9. Chronic inflammation and fibrosis (femur)	14	42	16.0	55.3	17.2
10. Hematoma, fat necrosis, and fibrosis	21	42	34.9	62.7	37.4
11. Chronic osteomyelitis (hip)	28	68	216.5	333.3	123.8
12. Mature ossification (soft tissue)	14	56	20.7	28.8	17.0
13. Fibrous dysplasia (femur)	10	119	125.5	431.0	56.8
14. Fibrous dysplasia (humerus)	7	42	75.8	92.0	81.4
15. Osteofibrous dysplasia	21	42	96.3	153.0	103.3
16. AVN of hip: right	28	105	79.9	128.7	38.0
left	21	56	39.9	80.0	28.5
17. Bone infarct	21	70	10.0	9.8	7.2
18. Compartment syndrome of calf	21	42	19.4	18.6	16.7
19. Fracture of hip	14	42	119.8	285.7	128.5
20. Fracture of fifth metatarsal	—	—	233.3	321.8	200.1
21. Stress fracture of tibia	0	84	171.0	310.3	97.7
22. Stress fracture of femur	21	28	105.7	146.9	151.0

TP = time to peak enhancement (seconds), TM = time to SI_{max} (seconds), PE = percent enhancement (%), RPeakE = rate of peak enhancement (%/minute), RE = rate of enhancement (%/minute), AVN = avascular necrosis.

Table 2
Malignant Conditions

	TP	TM	PE	RPeakE	RE
1. MFH 1	7	49	233.2	761.9	200.0
2. MFH 2	7	119	270.0	257.1	121.8
3. MFH 3	0	91	61.5	98.9	31.0
4. Liposarcoma	0	70	247.4	531.4	151.8
5. Lymphoma of femur	0	0	141.0	564.2	241.8
6. Lymphoma of wrist	7	16	160.0	643.7	342.9
7. Metastatic squamous cell cancer	—	—	236.2	191.5	112.5
8. Metastatic adenocarcinoma	0	0	271.3	775.5	775.5
9. Metastatic breast cancer	10	10	62.5	157.4	133.9
10. Synovial sarcoma	7	7	224.9	387.9	385.7
11. Chondrosarcoma (low gr.)	14	98	137	228.5	72.3
12. Chondrosarcoma (low gr.)	14	112	79.9	57.1	34.2
13. Osteosarcoma	14	56	146.6	342.8	114.2

TP = time to peak enhancement (seconds), TM = time to SI_{max} (seconds), PE = percent enhancement (%), RPeakE = rate of peak enhancement (%/minute), RE = rate of enhancement (%/minute), MFH = Malignant fibrous histiocytoma.
Note.—All lesions are pathologically proven.

Patients

A total of 35 patients were referred for MRI of musculoskeletal abnormalities. Patient age ranged from 10 to 81 years (mean, 43 years). There were 17 males and 18 females. Seventeen benign conditions were studied in 16 patients, 6 benign tumors were studied in 6 patients, and 13 malignant tumors were studied in 13 patients (Tables 1 and 2). Twenty-eight diagnoses were pathologically confirmed with surgical resection or lesional biopsy. The diagnosis of eight lesions (AVN, infarct, fractures, compartment syndrome) was established based on other imaging modalities and/or clinical follow-up or surgery (for the case of compartment syndrome).

Static MRI

MRI was performed at 1.5 T (Magnetom SP 4000, Siemens Medical Systems, Iselin, NJ) with the use of either a body, extremity, or surface coil, depending on the area of interest. Imaging was performed using T1-weighted SE, T2-weighted SE, or T2-weighted turbo (fast) SE, and/or turbo short-inversion-time inversion recovery (STIR), and/or FLASH gradient-echo sequences (Table 3). T1-weighted SE sequences were also performed after the dynamic contrast-enhanced study.

Dynamic Study

The dynamic study was performed using a gradient-echo sequence (TR = 33 msec, TE = 5 msec, flip angle [FA] = 80°, 256 × 144 matrix, 1 acquisition, 5- to 8-mm slice thickness) coupled with a fat-suppression pulse. Fat suppression was achieved by applying a presaturation pulse with a bandwidth of 220 Hz at an offset frequency optimized at the frequency of fat resonance. The optimum frequency was chosen in each case by inspecting images at various frequencies generated by a fat saturation tuning program. The frequencies were usually between −200 and −300 Hz. Immediately after the sequence was begun, a bolus of contrast material (gadopentetate dimeglumine, Berlex Laboratories, Cedar Knolls, NJ) was administered at a concentration of .1 mmol/kg over 10 seconds, followed immediately by a bolus injection of 10 ml of normal saline. One image was obtained every 7 seconds over a

Table 3
Range of Parameters for Static and Dynamic MRI

	TR (msec)	TE (msec)	Acquisitions	Thickness (mm)	FOV (mm)	Matrix
SE (T1)	200–670	14–15	1–3	3–8	230–500	192 × 256
SE (T2)	2,000–2,500	25/90–95	1–2	3–6	180–500	192 × 256
Turbo SE	2,850–4,800	21/91–103	2–3	3–5	200–450	174 × 512
Turbo STIR	2,600–3,800	18	1–3	3–6	230–500	192 × 512
GE (Static)	375–720	10–18	2–4	3–5	120–280	192 × 256
GE (Dynamic)	33	5	1	5–8	220–500	144 × 256

Turbo STIR: TI-150. GE (Static): flip angle = 30°, GE (Dynamic): flip angle = 80°. Turbo SE: echo train length (ETL) = 3, Echospace = 11.5 msec. Turbo STIR: ETL = 3, Echospace = 11.25 msec.
GE = Gradient echo.

Table 4
Range of Values Based on Classified Groups

	TP	TM	PE	RPeakE	RE
Benign tumors	0–56	0–119	62.3–169.0	52.7–142.8	29.6–142.8
Benign conditions	0–28	28–119	10.0–233.3	9.8–740.1	7.2–200.1
Malignant tumors	0–14	0–119	47–271.3	47.6–775.5	28.8–775.5
Fractures	0–21	28–84	105.7–233.3	146.9–321.8	97.7–200.1

TP = time to peak enhancement (seconds), TM = time to SI_{max} (seconds), PE = percent enhancement (%), RPeakE = rate of peak enhancement (%/minute), RE = rate of enhancement (%/minute).

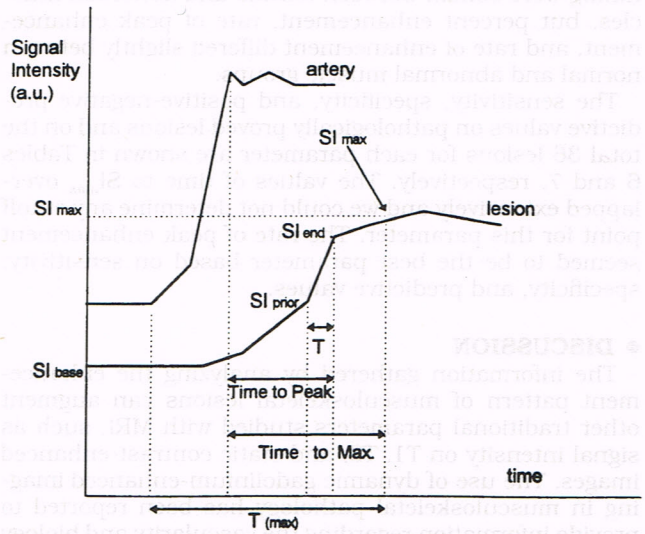

Figure 1. Image analysis. SI_{max} is the signal intensity at the time point at which the relative further signal increase between consecutive time points did not exceed 3% within the following 20 seconds. SI_{prior} and SI_{end} are the signal intensities at the time points at which the steepest part of the curve starts and ends, respectively. *T* is the time between SI_{prior} and SI_{end}. Time to peak enhancement is the time between the arterial peak enhancement and SI_{end}. Time to SI_{max} is the time between arterial peak enhancement and SI_{max}. SI_{base} is the signal intensity of a lesion before contrast injection. a.u.= arbitrary units.

period of 3.5 minutes (total number of images = 30). The contrast material was administered via a 20-gauge intravenous catheter that had been placed into an antecubital vein before positioning the patient in the magnet. As such, the patient was not moved at any time during the study. The imaging plane and imaging position were chosen from the precontrast images to include the central portion of the area of concern.

Image Analysis

The dynamic images at a given slice position were presented in a cine-loop format to assist in the visual identification of those areas showing maximum signal intensity (SI) changes. This allowed for a targeted region of interest (ROI) analysis. The ROI was selected to include the enhancing area but avoiding incorporation of subjacent tissue. The SI of the lesions and of an adjacent artery was measured over time in each of the images. For each tissue, the values were plotted against time. In an evaluation, the artery was considered the internal control, with time "0" considered the time when contrast appeared in the artery. For two lesions (fracture of fifth metatarsal and metastatic squamous cell carcinoma), an adjacent artery was not identified. SIs of other tissues, such as muscle, bone marrow, and fat, were also plotted against time. In the analysis of the dynamic images, we calculated five parameters (Fig. 1), according to these equations:

$$\text{Percent enhancement: } [(SI_{max} - SI_{base})/SI_{base}] \times 100\ (\%)$$

$$\text{Rate of peak enhancement: } [(SI_{end} - SI_{prior})/(SI_{base} \times T)] \times 100\ (\%/\text{minute})$$

$$\text{Rate of enhancement: } [(SI_{max} - SI_{base})/(SI_{base} \times T_{max})] \times 100\ (\%/\text{minute})$$

Time to peak enhancement: The time between the arterial peak enhancement and the end of the steepest portion of enhancement of pathologic tissue. As in the study by Erlemann et al (2,6,8), T_{max} is defined as the point at which the relative SI at T_{max} + 20 seconds is less than 3% higher than that at T_{max}.

Table 5
Mean Values Based on Classified Groups

	TP	TM	PE	RPeakE	RE
Benign tumors	18.5	64.5	102.4	118.3	80.1
Benign conditions	15.5	58.9	103.7	215.8	85.0
Malignant tumors	6.1	54.7	165.6	360.3	196.1
Fractures	11.6	51.3	157.4	266.1	144.3

TP = time to peak enhancement (seconds), TM = time to SI_{max} (seconds), PE = percent enhancement (%), RPeakE = rate of peak enhancement (%/minute), RE = rate of enhancement (%/minute).

Table 6
Sensitivity, Specificity, PPV, and NPV of Pathologically Proven Lesions for Malignant Tumors Based on the Best Cutoff Points

Parameters	Cutoff	Sensitivity (%)	Specificity (%)	PPV (%)	NPV (%)
Time to peak enhancement (seconds)	9	66.6	66.6	61.5	71.4
Percent enhancement (%)	135	76.9	73.3	71.4	78.5
Rate of peak enhancement (%/sec)	155	84.6	66.6	68.7	83.3
Rate of enhancement (%/sec)	105	76.9	66.6	66.6	76.9

Table 7
Sensitivity, Specificity, PPV, and NPV of All Lesions for Malignant Tumors Based on the Best Cutoff Points

Parameters	Cutoff	Sensitivity (%)	Specificity (%)	PPV (%)	NPV (%)
Time to peak enhancement (sec)	9	66.6	72.7	57.1	80.0
Percent enhancement (%)	135	76.9	73.9	62.5	85.0
Rate of peak enhancement (%/sec)	155	84.6	65.2	57.8	88.2
Rate of enhancement (%/sec)	105	76.9	65.2	55.5	83.3

Time to SI_{max}: The time between the arterial peak enhancement and the SI_{max}. The baseline value of the signal intensity (SI_{base}) was calculated on images that were acquired before the contrast enhancement was seen in the artery. SI end and SI prior values were those that differed most on the enhancement curve.

After all lesions were classified as benign tumor, benign non-neoplastic condition, malignant tumor, or fracture, the range of values and the mean values for the five parameters were calculated for each group (Tables 4 and 5). Based on the best cutoff points, sensitivity, specificity, and predictive values were calculated on the 28 pathologically proven lesions (Table 6) and on the total 36 lesions (Table 7). The cutoff points were determined as the points at which the highest sensitivity, specificity, and predictive values could be obtained.

• RESULTS

The time to peak enhancement, time to SI_{max}, percent enhancement, rate of peak enhancement, and rate of enhancement as determined for each condition are summarized in Tables 1 and 2. The range of values and the mean values for the five parameters are shown in Tables 4 and 5 for each group.

The mean values for the time to peak enhancement, percent enhancement, rate of peak enhancement, and rate of enhancement differed significantly between benign tumors and malignant tumors. On the other hand, the differences between malignant tumors and the other benign non-neoplastic conditions were less significant (Table 5).

Analysis of the enhancement curves demonstrated rapid enhancement of malignant tumors, which closely paralleled the enhancement profile of an adjacent artery (Fig. 2). The exceptions were two low grade chondrosarcoma and a case of osteosarcoma. Although benign conditions usually demonstrated a gradual enhancement over time in contrast to the intense and rapid enhancement of malignant tumors (Fig. 3), some benign conditions displayed a curve that virtually paralleled the arterial enhancement curve similar to malignant conditions (Figs. 4 and 5). The lesions that showed a rapid enhancement profile closely paralleling the adjacent artery were a giant cell tumor of tendon sheet, eosinophilic granuloma, and two fractures. Two enchondromas, a lymphohistiocytic granulomatous lesion, an intraosseous lipoma, and two fibrous dysplasia showed relatively rapid enhancement profiles.

In the case of bilateral AVN, the values on each side differed slightly. This was more significant for the values of time to SI_{max} and percent enhancement. In the case of compartment syndrome of the calf, the values of contrast timing were similar between normal and abnormal muscles, but percent enhancement, rate of peak enhancement, and rate of enhancement differed slightly between normal and abnormal muscle groups.

The sensitivity, specificity, and positive-negative predictive values on pathologically proved lesions and on the total 36 lesions for each parameter are shown in Tables 6 and 7, respectively. The values of time to SI_{max} overlapped extensively and we could not determine any cutoff point for this parameter. The rate of peak enhancement seemed to be the best parameter based on sensitivity, specificity, and predictive values.

• DISCUSSION

The information gathered by analyzing the enhancement pattern of musculoskeletal lesions can augment other traditional parameters studied with MRI, such as signal intensity on T1, T2, and static contrast-enhanced images. The use of dynamic gadolinium-enhanced imaging in musculoskeletal pathology has been reported to provide information regarding the vascularity and biology (malignant versus benign) of a lesion (1,7).

Several different techniques have been used to obtain dynamic contrast-enhanced images. In the two studies of Erlemann et al, a FLASH gradient-echo sequence (TR = 40 msec, TE = 10 msec, FA = 90°) was used for this purpose (2,6). Their technique allowed three sequence repetitions per minute. The percent and rate of enhancement (slope) was used to determine the vascularity and biology of musculoskeletal lesions. Accuracy rates of 83% and 86%, respectively, were acquired in these studies. Verstraete et al (1) used a turbo-FLASH gradient-echo sequence (TR = 9 msec, TE = 4 msec, TI = 200 msec, FA = 8°), which allowed for one slice in 1.41 seconds (1). In their study, the peak rate of enhancement was used as a parameter to determine the degree of vascularity of lesions at the steepest part of the enhancement curve, and secondary images (first pass images) were created based on the pixel's peak rate of enhancement values. The accuracy rate to determine the benign versus malignant nature of musculoskeletal lesions was found to be 76%. Moreover, there have been other studies in which slightly different techniques were used to assess the malignant lesion's response to chemotherapy and in assessing the

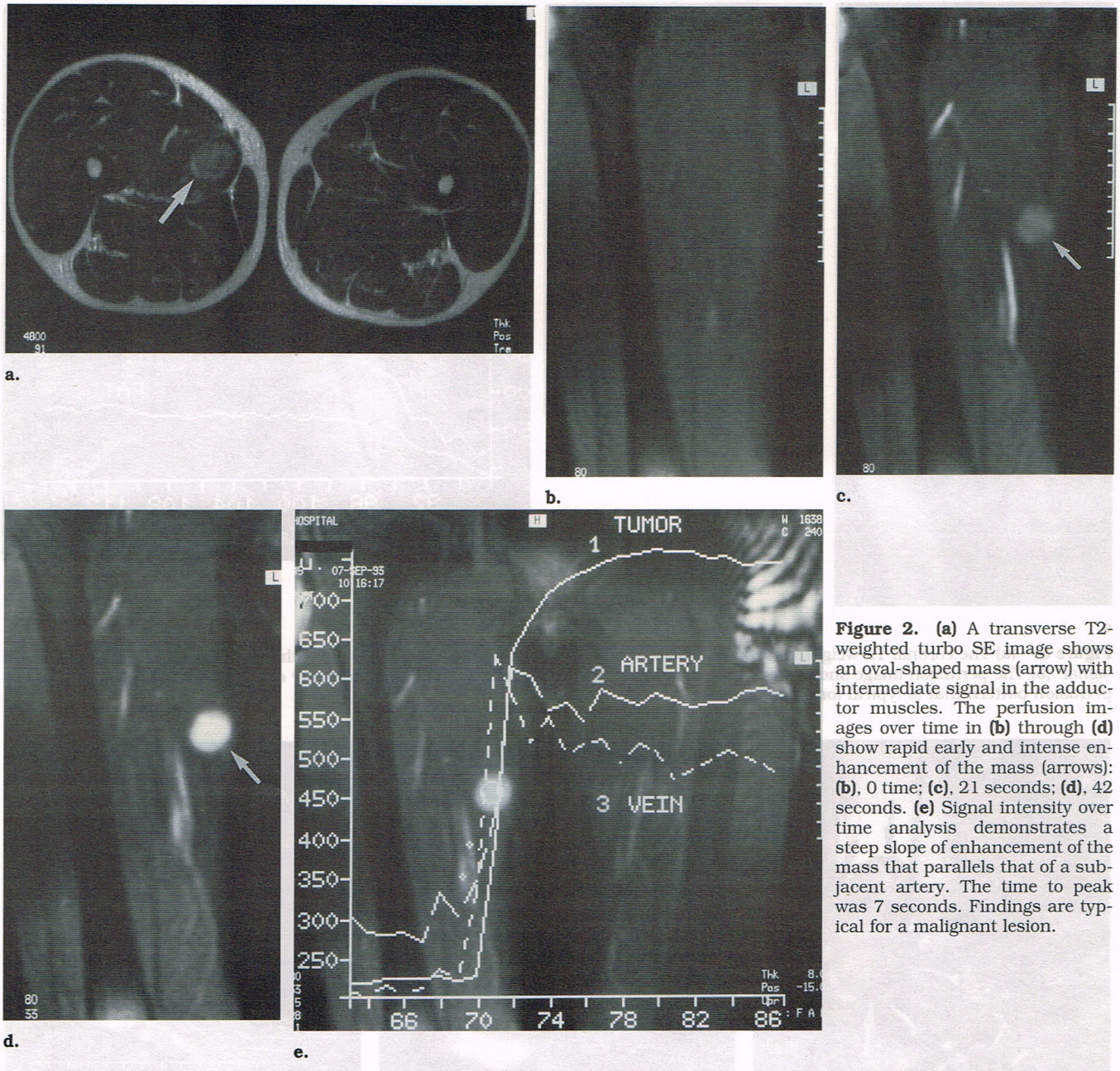

Figure 2. **(a)** A transverse T2-weighted turbo SE image shows an oval-shaped mass (arrow) with intermediate signal in the adductor muscles. The perfusion images over time in **(b)** through **(d)** show rapid early and intense enhancement of the mass (arrows): **(b)**, 0 time; **(c)**, 21 seconds; **(d)**, 42 seconds. **(e)** Signal intensity over time analysis demonstrates a steep slope of enhancement of the mass that parallels that of a subjacent artery. The time to peak was 7 seconds. Findings are typical for a malignant lesion.

enhancement dynamics of inflammatory disease such as rheumatoid arthritis (3,4,8,9,11,12).

In our study, a FLASH gradient-echo sequence was coupled with fat saturation, and a single slice was obtained every 7 seconds. This technique was relatively fast and allowed precise plotting of time-intensity curves. Studies of several investigators have shown that contrast-enhanced fat-suppression techniques improve the contrast between lesions and all adjacent mobile lipid and nonlipid-containing structures and greatly decrease or eliminate chemical shift artifacts (13–18). In our study, because of fat suppression, the contrast between the enhancing pathologic tissue and subjacent tissue was improved and lesions with high signal intensity due to paramagnetic relaxation enhancement were easily distinguished from low intensity fat. This eliminated the need for subtraction between pre- and post-contrast imaging. The elimination of subtraction also eliminated misregistration artifacts between precontrast and postcontrast images.

In previous studies, T_{max} was measured from the moment at which the bolus injection ended and dynamic scanning started. With those techniques, identical pathologic lesions could be enhanced with different times because of the different spatial locations of the lesions and inconsistent bolus injection rate. In our study, an adjacent artery in the imaging view was plotted against time. The use of an adjacent artery as an internal control was believed to be more reliable than other methods used in previous studies. The time at which contrast was seen in the artery was accepted as the reference time (time 0) to calculate the enhancement parameters. However, there were two cases in which an adjacent artery was not viewed. T_{max} was defined by Erlemann et al (8) as the time point at which the relative further signal increase between consecutive time points did not exceed 3% within the following 20 seconds. To compare our results with those of Erlemann et al, T_{max} and SI_{max} points were calculated based on Erlemann's definition.

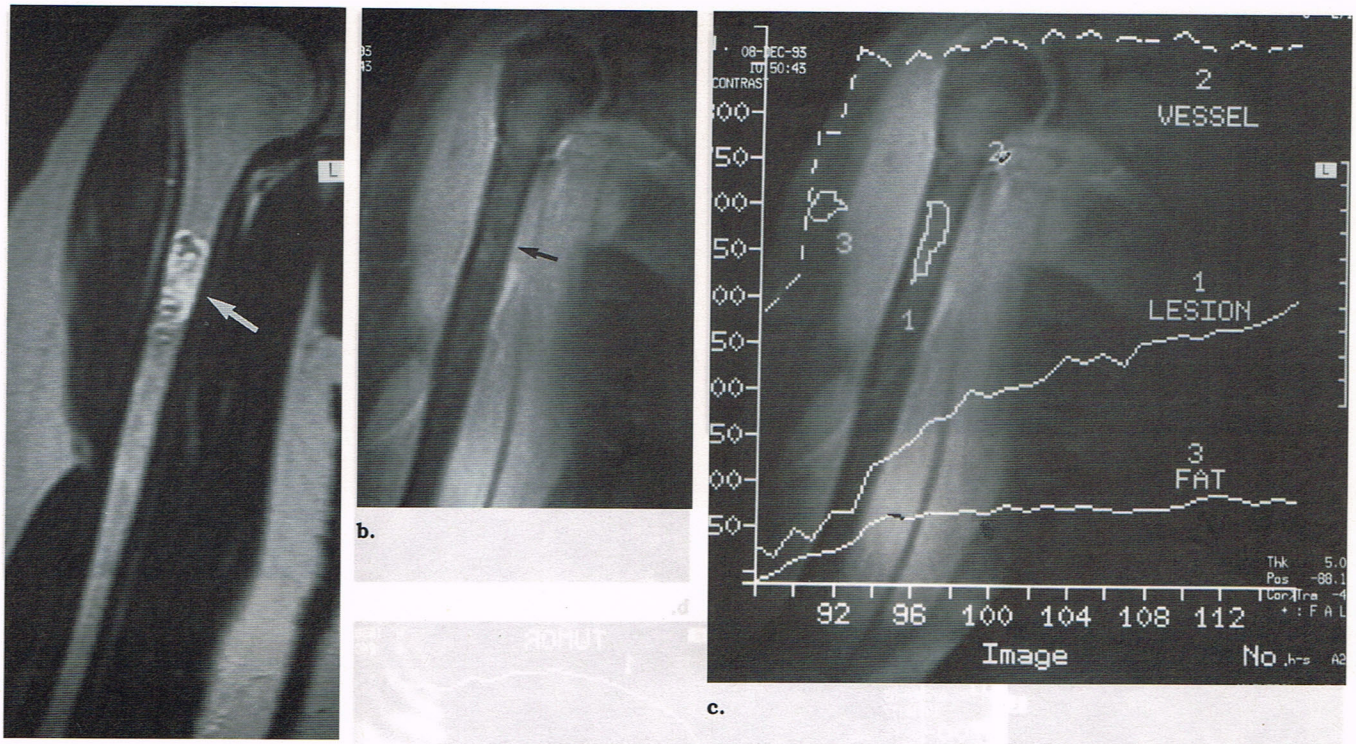

a. b. c.

Figure 3. **(a)** The coronal T2-weighted turbo SE image shows an intermedullary lesion (arrow) with increased signal and areas of low signal. **(b)** The perfusion image shows weak enhancement of the lesion (arrow). **(c)** Signal intensity over time analysis demonstrates a perfusion pattern that is typical for a benign lesion.

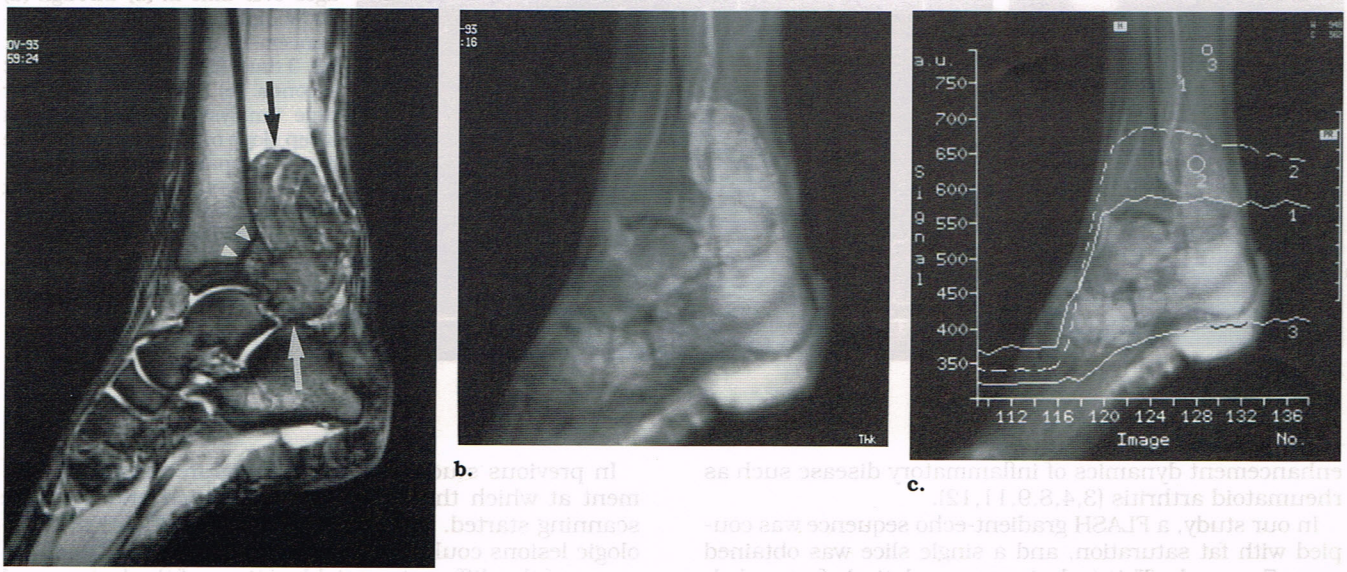

a. b. c.

Figure 4. Benign giant cell tumor of tendon sheet. **(a)** The sagittal T2-weighted gradient-echo image reveals a large, oval-shaped mass (arrows) near the Achilles tendon with heterogeneous signal and foci of low signal due to magnetic susceptibility effects of hemosiderin. There also is evidence for erosion into the tibia (arrowheads). **(b)** The perfusion image shows intense early enhancement of the mass. **(c)** Signal intensity over time analysis shows a peak enhancement close to that of an adjacent artery with a rapid slope of enhancement typical for malignant tumors.

In our study, based on the comparison among classified groups, the time to peak enhancement, percent enhancement, rate of peak enhancement and rate of enhancement differed significantly between benign and malignant conditions. These differences were especially clear between benign tumors and malignant tumors and were less significant among malignant tumors, fractures, and granulomatous lesions. On the other hand, the time to SI_{max} differed very slightly among all of these groups (Table 5).

In the study of Nadel et al (10), it was shown that there was no enhancement in the marrow cavity of the devascularized femoral heads in dogs (10). Our single case of

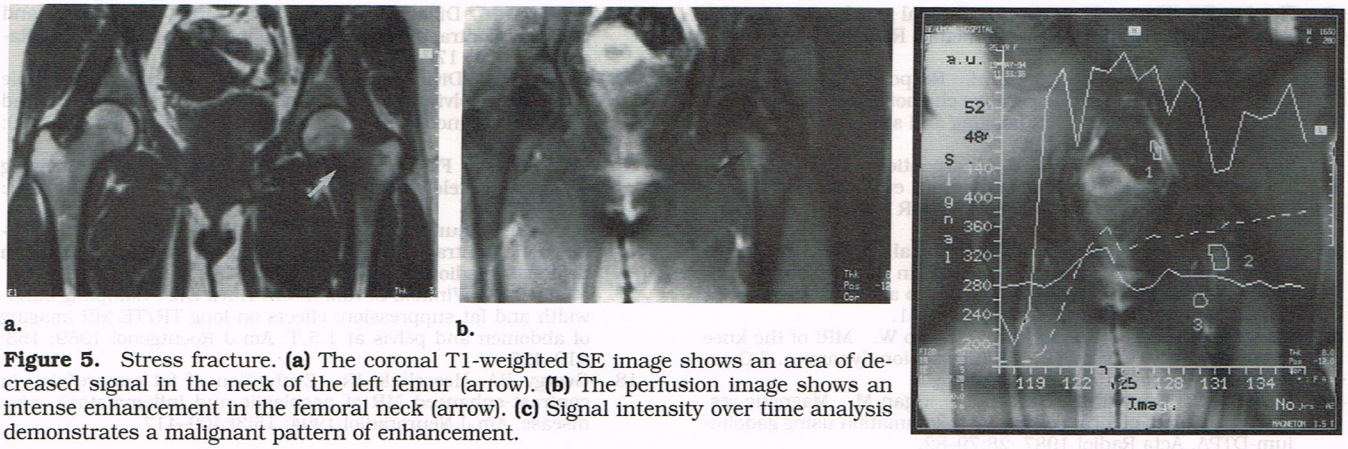

a. b. c.

Figure 5. Stress fracture. **(a)** The coronal T1-weighted SE image shows an area of decreased signal in the neck of the left femur (arrow). **(b)** The perfusion image shows an intense enhancement in the femoral neck (arrow). **(c)** Signal intensity over time analysis demonstrates a malignant pattern of enhancement.

bilateral AVN showed enhancement, although it was much less than benign conditions (right: percent enhancement = 79.9%, rate of enhancement = 38.09%/minute; left: percent enhancement = 39.9%, rate of enhancement = 28.5%/minute). These differences of enhancement were believed to be due to the presence of the reparative process in different stages.

Despite the promising results based on the mean values, there were significant overlaps between malignant tumors and benign conditions. Analysis of our data showed that the rate of peak enhancement, percent enhancement, and rate of enhancement parameters gave comparable results and that the best parameter was the rate of peak enhancement, with a 155%/minute cutoff point (sensitivity: 84.6%, specificity: 65.2–66.6%, positive predictive value [PPV]: 57.8–68.7%, negative predictive value [NPV]: 83.3–88.2%). The percent enhancement, rate of enhancement, and time to peak enhancement parameters had slightly lower accuracy rates (Tables 6 and 7).

In the studies by Erlemann et al (2,6,8), the cutoff point was 30%/minute for the rate of enhancement (slope value). When we applied the 30%/minute cutoff point, the sensitivity became 100%; however, the specificity of this technique was only 18.7% because there were several benign conditions that showed a higher rate of enhancement than this cutoff point. Our results in this retrospective study parallel the study by Fletcher and Hanna (7). Their study histologically proved that all seven benign conditions, including tumors such as enchondroma and neurofibroma, had higher than 30%/minute rates of enhancement as well. Erlemann explained Fletcher's results by the use of a 40° FA and a 1.0-T magnet (7). We used a TR, TE, and FA similar to the study of Erlemann et al with a 1.5-T magnet and only 5 of 23 benign lesions showed less than 30%/minute rate of enhancement. Our T_{max} values probably were shorter than those of Erlemann et al because of the use of an adjacent artery as an internal control.

Although analysis of the enhancement curves has shown that malignant tumors usually show rapid enhancement, which closely parallels that of an adjacent artery, there were several benign lesions (giant cell tumor of tendon sheet, eosinophilic granuloma, and fractures) with a similar enhancement patterns. In addition, several other benign lesions, such as enchondroma, lymphohistiocytic granulomatous lesion, intraosseous lipoma, osteomyelitis, and fibrous dysplasia, showed relatively rapid enhancement profile. The sensitivity and specificity values of these two parameters (time to peak enhancement and time to SI_{max}) verify this result. Our results demonstrated lower sensitivity and specificity as compared with previous studies; however, our technique may be more reliable with fat suppression coupled with the timing of parameters relative to the enhancement of an adjacent artery. The best parameters to classify the nature of musculoskeletal lesions were rate of peak enhancement, percent enhancement, and rate of enhancement. The results based on time to peak enhancement seem less successful and the least reliable parameter was the time to SI_{max}.

Limitations of this study include a relatively small number of patients and, in some examinations, insufficient fat suppression, which was seen in studies requiring a large field of view (FOV). Nevertheless, certain trends were identified by using this modified technique for dynamic imaging.

In conclusion, the dynamic gradient echo (FLASH) contrast-enhanced fat-saturation sequence can be used successfully in this field. The rate of peak enhancement seemed to be the best parameter for distinguishing malignant lesions from benign conditions. Although the other parameters (percent enhancement, rate of enhancement, and time to peak enhancement) seemed less successful, similar results were obtained. However, because of a significant overlap between malignant tumors and benign conditions in our study, accuracy rates seem lower than reported previously.

References

1. Verstraete KL, Deene YD, Roels H, Dierick A, Uyttendaele D, Kunnen M. Benign and malignant musculoskeletal lesions: dynamic contrast-enhanced mr imaging — parametric "first-pass" images depict tissue vascularization and perfusion. Radiology 1994; 192:835–843.
2. Erlemann R, Reiser MF, Peters PE, et al. Musculoskeletal neoplasms: static and dynamic Gd DTPA-enhanced MR imaging. Radiology 1989; 171:767–773.
3. Fletcher BD, Hanna SL, Fairclough DL, Gronemeyer SA. Pediatric musculoskeletal tumors: use of dynamic contrast-enhanced MRI imaging to monitor response to chemotherapy. Radiology 1992; 184:243–248.
4. Bonnerot V, Charpentier A, Frovin F, Kalifa C, Vanel D, Paola RD. Factor analysis of dynamic magnetic resonance imaging in predicting response of osteosarcoma to chemotherapy. Invest Radiol 1992; 27:847–855.
5. Hanna SL, Parham DM, Fairclough DL, Meyer WH, Le AH, Fletcher BD. Assessment of osteosarcoma response to preoperative chemotherapy using dynamic FLASH gadolinium-DTPA-enhanced magnetic resonance imaging. Invest Radiol 1992; 27:367–373.
6. Erlemann R, Sciuk J, Wuisman P, et al. Dynamic MR tomography in the diagnosis of inflammatory and tumorous space-occupying lesions of the musculoskeletal system. Rofo Fortschr Geb Rontgenstr Neuen Bildgeb Verfahr 1992; 156:353–359.

7. Fletcher BD, Hanna SL. Musculoskeletal neoplasms: dynamic Gd-DTPA enhanced MR imaging. (letter) Radiology 1990; 177: 287–288.
8. Erlemann R, Sciuk J, Bosse A, et al. Response of osteosarcoma and Ewing sarcoma to preoperative chemotherapy: assessment with dynamic and static MR imaging and skeletal scintigraphy. Radiology 1990; 175:791–796.
9. Baere T, Vanel D, Shapeero GL, Charpentier A, Terrier P, Paola M. Osteosarcoma after chemotherapy: evaluation with contrast material-enhanced subtraction MR imaging. Radiology 1992; 185:587–592.
10. Nadel SN, Debatin JF, Richardson WJ, et al. Detection of acute avascular necrosis of the femoral head in dogs: dynamic contrast-enhanced MR imaging vs spin-echo and STIR sequences. Am J Roentgenol 1992; 159(6):1255–1261.
11. Yamoto M, Tamai K, Yamaguchi T, Ohno W. MRI of the knee in rheumatoid arthritis: Gd-DTPA perfusion dynamics. J Comput Assist Tomogr 1993; 17(5):781–785.
12. Paajanen H, Brasch RC, Schmiedl U, Ogan M. Magnetic resonance imaging of local soft tissue inflammation using gadolinium-DTPA. Acta Radiol 1987, 28:79–82.
13. Barakos JA, Dillon WP, Chew WM. Orbit, skull base, and pharynx: contrast-enhanced fat suppression MR imaging. Radiology 1991; 179:191–198.
14. Rahmouni A, Divine M, Mathieu D, et al. Detection of multiple myeloma involving the spine: efficacy of fat- suppression and contrast-enhanced MR imaging. Am J Roentgenol 1993; 160: 1049–1052.
15. Mirowitz SA. Fast scanning and fat-suppression MR imaging of musculoskeletal disorders. Am J Roentgenol 1993; 161: 1147–1157.
16. Simon JH, Szumowski J. Chemical shift imaging with paramagnetic contrast material enhancement for improved lesion depiction. Radiology 1989; 171:539–543.
17. Mitchell DG, Vinitski S, Rifkin MD, Burk DL. Sampling bandwidth and fat suppression: effects on long TR/TE MR imaging of abdomen and pelvis at 1.5 T. Am J Roentgenol 1989; 153: 419–425.
18. Georgy BA, Hesselink JR. Evaluation of fat suppression in contrast-enhanced MR of neoplastic and inflammatory spine disease. Am J Neuroradiol 1994; 15(3):409–417.